

1 **The Dual-Antigen Ad5 COVID-19 Vaccine Delivered as an Intranasal Plus Subcutaneous**
2 **Prime Elicits Th1 Dominant T-Cell and Humoral Responses in CD-1 Mice**

3
4 Adrian Rice¹ϕ, Mohit Verma¹ϕ, Annie Shin¹, Lise Zakin¹, Peter Sieling¹, Shiho Tanaka¹, Joseph
5 Balint¹, Kyle Dinkins¹, Helty Adisetiyo¹, Brett Morimoto¹, Justin Taft^{2,3}, Roosheel Patel^{2,3},
6 Sofija Buta^{2,3,4}, Marta Martin-Fernandez^{2,3,4,5,6}, Dusan Bogunovic^{2,3,4,5,6}, Patricia Spilman¹,
7 Elizabeth Gabitzsch¹, Jeffrey T. Safrit¹, Shahrooz Rabizadeh¹, Kayvan Niazi¹, Patrick Soon-
8 Shiong¹*

9
10 ϕ These authors contributed equally

11 ¹ImmunityBio, Inc., 9920 Jefferson Blvd, Culver City, CA 90232, USA

12 ²Center for Inborn Errors of Immunity, ³Department of Pediatrics, ⁴Precision Immunology
13 Institute, ⁵Mindich Child Health and Development Institute, ⁶Department of Microbiology,
14 Icahn School of Medicine at Mount Sinai, 1 Gustave Lane, Levy Place, New York, NY 10029-
15 5674, USA

16
17 *Corresponding author: Patrick@NantWorks.com

18

19

20

21

22

23

24

25 **ABSTRACT**

26 In response to the need for an efficacious, thermally-stable COVID-19 vaccine that can elicit
27 both humoral and cell-mediated T-cell responses, we have developed a dual-antigen human
28 adenovirus serotype 5 (hAd5) COVID-19 vaccine in formulations suitable for subcutaneous (SC),
29 intranasal (IN), or oral delivery. The vaccine expresses both the SARS-CoV-2 spike (S) and
30 nucleocapsid (N) proteins using an hAd5 platform with E1, E2b, and E3 sequences deleted
31 (hAd5[E1-, E2b-, E3-]) that is effective even in the presence of hAd5 immunity. In the vaccine, S
32 is modified (S-Fusion) for enhanced cell-surface display to elicit humoral responses and N is
33 modified with an Enhanced T-cell Stimulation Domain (N-ETSD) to direct N to the
34 endosomal/lysosomal pathway to increase MHC I and II presentation. Initial studies using
35 subcutaneous (SC) prime and SC boost vaccination of CD-1 mice demonstrated that the hAd5 S-
36 Fusion + N-ETSD vaccine elicits T-helper cell 1 (Th1) dominant T-cell and humoral responses to
37 both S and N. We then compared SC to IN prime vaccination with either an SC or IN boost post-
38 SC prime and an IN boost after IN prime. These studies reveal that IN prime/IN boost is as
39 effective at generating Th1 dominant humoral responses to both S and N as the other combinations,
40 but that the SC prime with either an IN or SC boost elicits greater T cell responses. In a third study
41 to assess the power of the two routes of delivery when used together, we used a combined SC plus
42 IN prime with or without a boost and found the combined prime alone to be as effective as the
43 combined prime with either an SC or IN boost in generating both humoral and T-cell responses.
44 The findings here in CD-1 mice demonstrate that combined SC and IN prime-only delivery has
45 the potential to provide broad immunity – including mucosal immunity – against SARS-CoV-2
46 and supports further testing of this delivery approach in additional animal models and clinical
47 trials.

48

49

50 INTRODUCTION

51 In response to the need for a COVID-19 vaccine that is safe, effective, and suitable for global
52 distribution, we have developed the dual antigen hAd5 S-Fusion + N-ETSD vaccine including
53 formulations for subcutaneous (SC), oral, and intranasal (IN) delivery. The vaccine comprises the
54 SARS-CoV-2 spike (S) protein optimized for cell surface expression (S-Fusion)¹ to increase
55 humoral responses and the nucleocapsid protein with an Enhanced T-cell Stimulation Domain (N-
56 ETSD) to target N to the endosomal/lysosomal cellular compartment to enhance MHC I and II
57 presentation.²

58 The vaccine antigens are delivered using a human adenovirus serotype 5 (hAd5) vector with
59 deletions in the E1, E2b, and E3 gene regions (hAd5 [E1-, E2b-, E3-]; Supplementary Fig. S1A).³
60 Specifically, removal of the E2b regions confers advantageous immune properties by minimizing
61 immune responses to Ad5 viral proteins such as viral fibers,⁴ thereby eliciting potent immune
62 responses to specific antigens in patients with pre-existing adenovirus (Ad) immunity.^{5,6} Since
63 these deletions allow the hAd5 platform to be efficacious even in the presence of existing Ad
64 immunity, this platform enables relatively long-term antigen expression without significant
65 induction of anti-vector immunity. It is therefore also possible to use the same vector/construct for
66 homologous prime-boost therapeutic regimens.⁷ Importantly, this next generation Ad vector has
67 demonstrated safety in over 125 patients with solid tumors. In these Phase I/II studies, CD4+ and
68 CD8+ antigen-specific T cells were successfully generated to multiple somatic antigens (CEA,
69 MUC1, brachyury) even in the presence of pre-existing Ad immunity.^{5 8}

70 SARS-CoV-2 is an enveloped positive sense, single-strand RNA β coronavirus primarily
71 composed of four structural proteins - spike (S), nucleocapsid (N), membrane (M), and envelope
72 (E) – as well as the viral membrane and genomic RNA. The S glycoprotein⁹⁻¹¹ is displayed as a
73 trimer on the viral surface, whereas N is located within the viral particle (Supplementary Fig. S1B).

74 Spike initiates infection by the SARS-CoV-2 virus by interaction of its receptor binding domain
75 (RBD) with the human host angiotensin-converting enzyme 2 (ACE2) expressed on the surface of
76 cells in the respiratory system, including alveolar epithelial cells,¹² as well as cells in the digestive
77 tract.

78 The majority of current SARS-CoV-2 vaccines under development deliver only the S antigen
79 because antibodies raised against S RBD are expected to neutralize infection.¹³⁻¹⁵ Reliance on S as
80 the sole vaccine antigen is not without risk, however, particularly in the face of the rapidly
81 dominating variants including the B.1.351 variant expressing E484K, K417N, and N501Y
82 mutations;¹⁶ the B.1.1.7 variant (N501Y);^{17,18} and the Cal.20.C L452R variant¹⁹ all of which
83 have altered RBD sequences that may not be as effectively recognized by antibodies generated in
84 response to first-wave S-based vaccines.

85 To lessen the risk of single-antigen delivery and to broaden protective immune responses, we
86 included the N protein in our hAd5 S-Fusion + N-ETSD vaccine (Supplementary Fig. S1C). N is
87 a highly conserved and antigenic SARS-CoV-2-associated protein that has been studied previously
88 as an antigen in coronavirus vaccine design for SARS-CoV.²⁰⁻²³ N associates with viral RNA and
89 has a role in viral RNA replication, virus particle assembly, and release.^{24,25} Studies have shown
90 that nearly all patients infected with SARS-CoV-2 have antibody responses to N.^{26,27} Furthermore,
91 another study reported that most, if not all, COVID-19 survivors tested were shown to have N-
92 specific CD4+ T-cell responses.¹⁵

93 The ability of N to elicit vigorous T-cell responses highlights another advantage of the addition
94 of N. A robust T-cell response to vaccination is at least as important as the production of antibodies
95²⁸ and should be a critical consideration for COVID-19 vaccine efficacy. First, humoral and T-cell
96 responses are highly correlated, with titers of neutralizing antibodies being proportional to T-cell
97 levels, suggesting the T response is necessary for an effective humoral response.²⁹ It is well

98 established that the activation of CD4+ T helper cells enhances B-cell production of antibodies.
99 Second, virus-specific CD4+ and CD8+ T cells are widely detected in COVID-19 patients,³⁰ based
100 on findings from patients recovered from the closely-related SARS-CoV, and there are reports that
101 such T cells persist for at least 6–17 years, suggesting that T cells may be an important part of
102 long-term immunity.³¹⁻³³ These T-cell responses were predominantly to N, as described in Le Bert
103 *et al.*, who found that in all 36 convalescent COVID-19 patients in their study, the presence of
104 CD4+ and CD8+ T cells recognizing multiple regions of the N protein could be demonstrated.³³
105 They further examined blood from 23 individuals who had recovered from SARS-CoV and found
106 that the memory T cells acquired 17 years ago also recognized multiple proteins of SARS-CoV-2.
107 These findings emphasize the importance of designing a vaccine with the highly conserved
108 nucleocapsid present in both SARS-CoV and SARS-CoV-2. Third, recovered patients exposed to
109 SARS-CoV-2 have been found without seroconversion, but with evidence of T-cell responses.³⁴
110 The T-cell based responses become even more critical given the finding in at least one study that
111 neutralizing antibody titers decline in some COVID-19 patients after about 3 months.³⁵ The
112 importance of both S and N was highlighted by Grifoni *et al.*¹⁵ who identified both S and N
113 antigens as *a priori* potential B and T-cell epitopes for the SARS-CoV virus that shows close
114 similarity to SARS-CoV-2 that are predicted to induce both T and B cell responses.

115 Additional considerations for vaccine design beyond the choice of antigens, include the
116 practicality of global distribution and the ability to generate mucosal immunity that provides the
117 highest probability of preventing transmission. While the mRNA-based vaccines have shown
118 excellent efficacy,^{36,37} their requirement for extremely cold storage has presented a challenge,
119 particularly for developing countries. Our hAd5 [E1-, E2b-, E3-] platform-based vaccine
120 overcomes the need for super-cold storage, with the injectable and IN formulations requiring only

121 -20°C (up to one year) or 2-8°C (up to one month) storage. The oral formulation has a further
122 advantage of being stable at room temperature.

123 IN or oral vaccine delivery also offers the potential for conferring mucosal immunity. SARS-
124 CoV-2 is a mucosal virus^{38,39} that in most instances of infections, initiates infection by entry to
125 the nose and mouth. Similarly, it's most efficient route of transmission is by respiratory droplets
126 that are then transmitted to other persons.⁴⁰ Thus a vaccine that also elicits protective mucosal
127 responses mediated by IgA is more likely to reduce transmission as compared to systemic, IgG-
128 only humoral and T-cell responses.⁴¹

129 It was our goal in the studies presented herein to confirm enhanced cell surface expression of
130 S-Fusion as compared to S-WT (the localization of N-ETSD to endo/lysosomes is demonstrated
131 in Sieling *et al.* 2020²) in *in vitro* studies, then assess humoral and T cell responses *in vivo* studies
132 in CD-1 mice. In mice, first the immune responses to SC prime and SC boost vaccination were
133 determined, then SC and IN prime delivery were compared. In a third experiment, the two routes
134 of delivery were combined in a single boost to ascertain if together optimal immune responses
135 could be achieved that may not necessarily be dependent upon a boost.

136 In all three study paradigms - SC prime with SC boost study, SC versus IN prime with boost,
137 and combined SC plus IN prime with or without boost - immunization of CD-1 mice with the hAd5
138 S Fusion + N-ETSD vaccine elicited Th1 dominant, virus-neutralizing humoral responses against
139 S. Both CD4+ and CD8+ T-cell responses to SARS-CoV-2 S and N peptide pools were also seen,
140 with cytokine production being greater overall in response to N peptides in all studies. Potent
141 neutralization of SARS-CoV-2 by sera from vaccinated mice in all studies was confirmed by a
142 surrogate neutralization assay.⁴² While all dosing paradigms produced broad immune responses,
143 perhaps the most significant and compelling finding was that a single prime administration by

144 combined SC and IN dosing generated immune responses that were at least as great as dosing
145 regimens that included a boost.

146

147 **RESULTS**

148 **S-Fusion enhances cell-surface display of conformationally-relevant spike**

149 Before initiation of *in vivo* studies in mice, our goal of enhancing cell-surface display of S was
150 confirmed by transfection of HEK-293T cells with hAd5 S wild type (S WT), S-WT plus N-ETSD,
151 S-Fusion alone, and S-Fusion plus N-ETSD followed by flow cytometric analysis of anti-S
152 receptor binding domain (S RBD) antibody binding. As shown in Supplementary Figure S2A-E,
153 antibody binding was enhanced with S-Fusion as compared to S-WT and was found to be the
154 highest for hAd5 S-Fusion plus N-ETSD. This enhanced cell surface expression was further
155 confirmed by binding of recombinant ACE2, which was also the highest for hAd5 S-Fusion + N-
156 ETSD (Supplementary Fig. S2F-H). The binding of both antibodies and ACE2 to S as expressed
157 by the vaccine not only confirms increased surface expression, it verifies conformational relevance
158 of the surface-displayed S protein.

159 ***In Vivo* Studies in Mice**

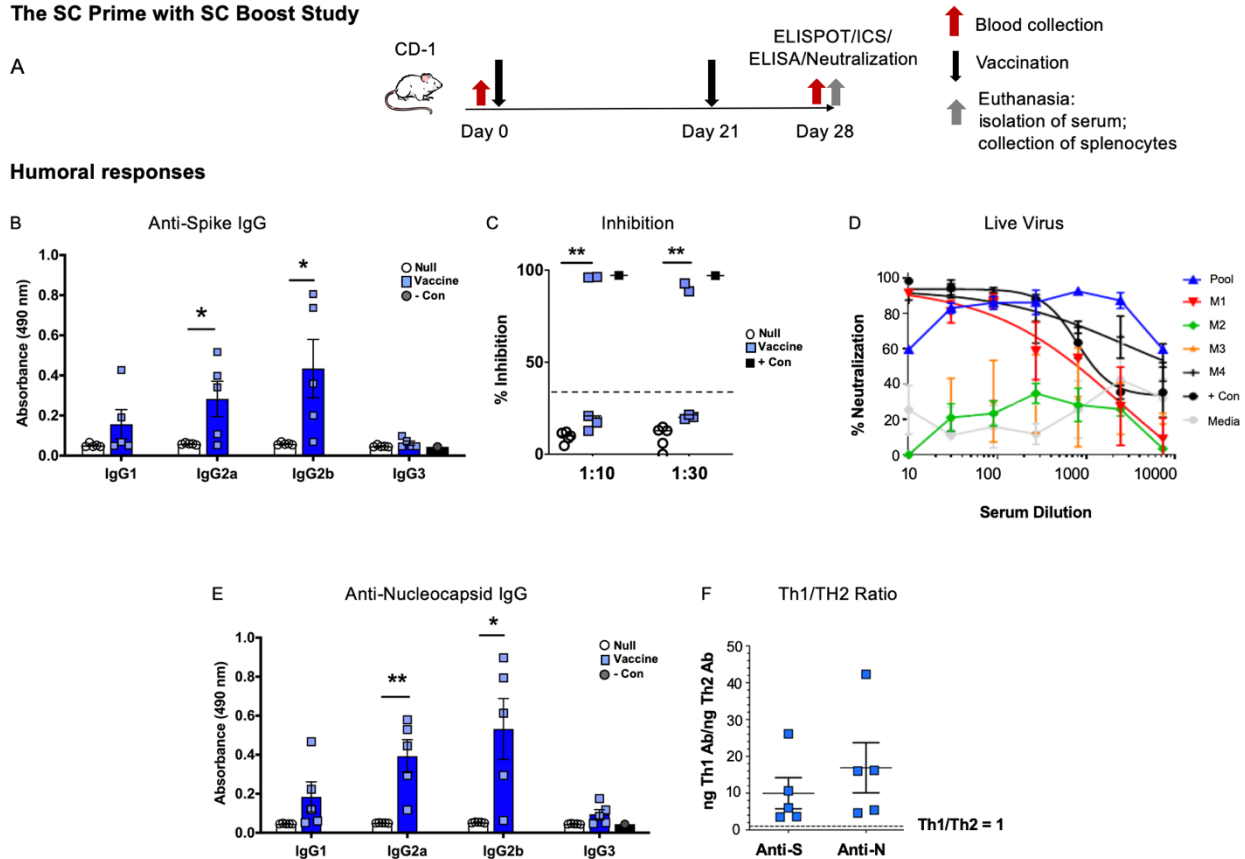
160 **Mice generated both anti-S and anti-N antibodies in response to SC prime, SC boost** 161 **vaccination**

162 In this study to test an SC hAd5 S-Fusion + N-ETSD prime followed by an SC boost, CD-1
163 female mice received 1×10^{10} viral particles (VP) of either hAd5 Null or the vaccine, both $n = 5$,
164 on Days 0 and 21. Mice were euthanized and tissue collected for analysis on Day 28 (Fig. 1A).

165 Vaccinated mice generated anti-S antibodies that were shown to be neutralizing in surrogate
166 and live virus assays (Fig. 1B, C, and D, respectively). Vaccinated mice also generated anti-N
167 antibodies (Fig. 1E), and both the anti-S and anti-N antibodies were Th1 dominant (Fig. 1F).

168 Our neutralization data with live SARS-CoV-2 virus demonstrated the potency of the antibody
 169 response generated following vaccination with hAd5 S-Fusion + N-ETSD, with evidence of high
 170 neutralization even at a high dilution factor. In addition, a synergistic effect of pooled sera was
 171 evident, with potent neutralization even greater than control convalescent serum at $\geq 1:1,000$
 172 dilution.

The SC Prime with SC Boost Study



173 **Fig. 1** Humoral responses in the SC prime, SC boost study. (A) CD-1 mice received either hAd5
 174 Null or the hAd5 S-Fusion + N-ETSD vaccine (both n = 5) on Day 0 and Day 21 by subcutaneous
 175 (SC) injection and were euthanized for tissue collection on Day 28. (B) Anti-spike (S) antibody
 176 levels in sera by isotype are shown (dilution 1:30); (C) results of the surrogate spike receptor
 177 binding domain (S RBD): angiotensin-converting enzyme 2 (ACE2) binding assay where
 178 inhibition of 35% or greater is associated with neutralization; and (D) percent neutralization in the
 179 live virus assay are shown for the 4 vaccinated mice with assessable sera as well as pooled sera
 180 from these mice. (E) Anti-nucleocapsid (N) antibody levels (dilution 1:90) by isotype and (F) the
 181 T helper cell 1 (Th1)/Th2 ratios for both anti-S and anti-N antibodies with a ratio greater than 1
 182 representing Th1 dominance. Statistics performed using an unpaired two-tailed Student's t-test
 183 where *p < 0.05 and **p ≤ 0.01.

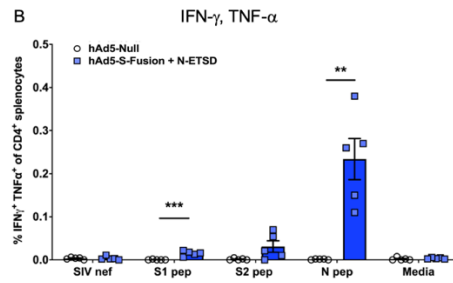
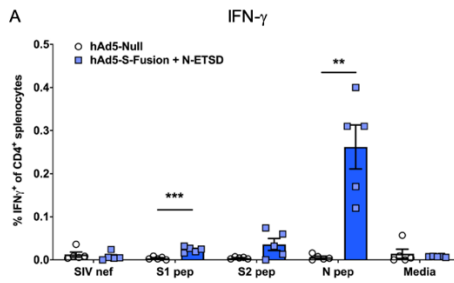
185

186 **N peptides elicited strong CD4⁺ T-cell, but S peptides elicited strong CD8⁺ T-cell responses**
187 **in SC prime, SC boost vaccinated mice**

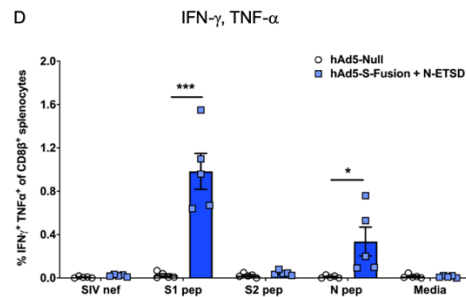
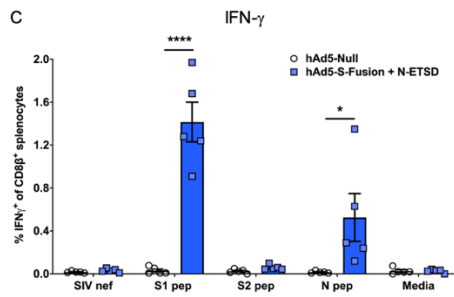
188 Intracellular cytokine staining (ICS) revealed that the N peptide pool stimulated interferon- γ
189 (IFN- γ) and tumor necrosis factor alpha (TNF- α) production in selected CD4⁺ T-lymphocytes
190 from vaccinated but not hAd5 Null mice (Fig. 2A and B). Conversely, the S1 peptide pool
191 (containing S RBD) elicited higher IFN- γ /TNF- α production in CD8⁺ T-lymphocytes than the N
192 peptide pool (Fig. 2C and D). ELISpot showed N peptides stimulated higher IFN- γ secretion than
193 the S1 peptide pool, but cytokine secretion was greater with both stimuli in T-cells from vaccinated
194 mice as compared to Null (Fig. 2E). IL-4 secretion was very low, therefore the T-cell responses,
195 like humoral responses, were Th1 dominant with the IFN- γ /IL-4 ratio being >1 in 4 of 5 vaccinated
196 mice (Fig. 2F and G).

The SC Prime with SC Boost Study: T-Cell Responses

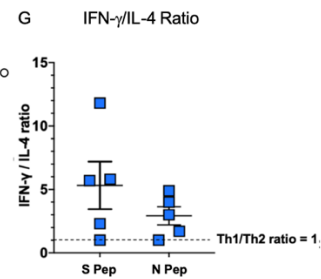
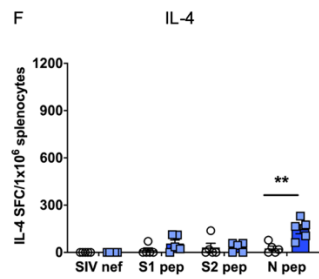
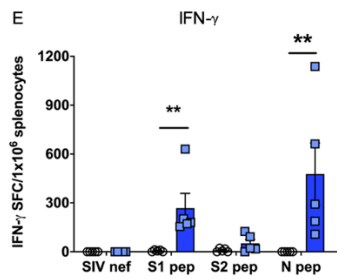
CD4+ ICS



CD8+ ICS



ELISpot



197
 198 **Fig. 2** T-cell responses in SC prime, SC boost hAd5 S-Fusion + N-ETSD vaccinated mice.
 199 Production of interferon- γ (IFN- γ) for (A) CD4+ and (C) CD8 β + T lymphocytes; and IFN- γ /tumor
 200 necrosis factor α (TNF- α) by (B) CD4+ and (D) CD8 β + T lymphocytes by intracellular cytokine
 201 staining (ICS) is shown. ELISpot detection of (E) IFN- γ and (F) interleukin-4 (IL-4) by T-
 202 lymphocytes is shown. In both ICS and ELISpot, cytokine production is stimulated by exposure
 203 to S1, S2 or N peptide pools; media only and SIV nef are negative controls. (G) The IFN- γ /IL-4
 204 ratio > 1 reflects Th1 dominance. Statistical analyses performed using an unpaired, two-tailed
 205 Student's t-test where * $p < 0.05$, ** $p \leq 0.01$, and *** $p \leq 0.001$.

206
 207 **IN prime with an IN boost vaccination with hAd5 S-Fusion + N-ETSD elicited humoral**
 208 **responses that were as good or better than SC prime with either SC or IN boost**

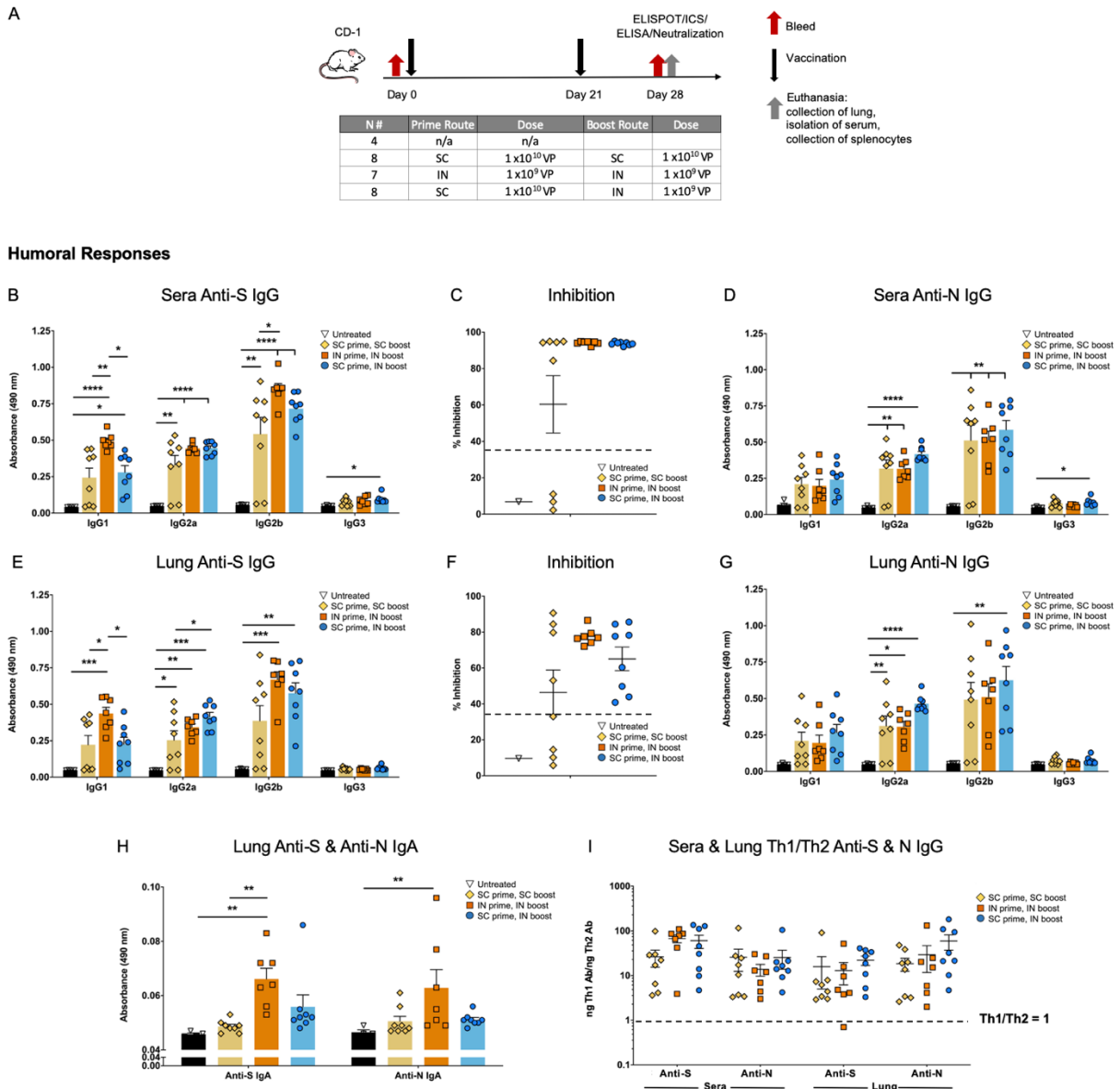
209 To both enhance and broaden immune responses by generation of mucosal immunity, we next
 210 performed a study wherein the prime delivery by either SC and intranasal (IN) routes would be
 211 compared when followed by either an SC or IN boost. The design of the SC versus IN prime with

212 SC or IN boost study is shown in Figure 3A. There were 4 groups of CD-1 mice: untreated, SC
213 prime followed by SC boost (SC > SC), IN prime followed by IN boost (IN > IN), and SC prime
214 followed by IN boost (SC > IN). SC doses were administered at 1×10^{10} VP and IN doses were
215 administered at 1×10^9 VP. The untreated group was $n = 4$, SC > SC and SC > IN were $n = 8$ and
216 IN > IN $n = 7$. Mice received the priming doses on Day 0 and boosting doses on Day 21. All mice
217 were euthanized on Day 28 and tissue including blood for serum, spleens for T cells, and lung
218 tissue collected for analyses.

219 Mice in all vaccinated groups produced anti-S IgG and overall, levels were the highest in sera
220 from IN > IN group mice (Fig. 3B). Sera were highly neutralizing as reflected by high inhibition
221 in the surrogate virus neutralization assay (Fig. 3C). Anti-N IgG was also detected in sera from all
222 vaccinated mice, with the levels being very similar between vaccinated groups (Fig. 3D).

223 Similar to the findings for sera, anti-S IgG was detected in lung homogenate of all vaccinated
224 mice and was higher overall for the IN > IN group (Fig. 3E). Lung homogenate from all IN > IN
225 group mice showed high inhibition in the surrogate neutralization assay, whereas homogenate from
226 4 mice in the SC > SC boost group did not surpass the 35% level of inhibition that is associated
227 with viral neutralization (Fig. 3F). In lung homogenate, anti-N IgG showed a trend to higher in the
228 SC > IN group (Fig. 3G). Not unexpectedly, both anti-S and anti-N IgA levels in lung homogenate
229 were highest in the IN > IN boost group (Fig. 3H). Furthermore, the anti-S and anti-N responses
230 in both sera and lung were highly Th1 dominant for all vaccinated groups (Fig. 3I).

The SC versus IN Prime with IN or SC Boost Study



231
 232 **Fig. 3** Humoral responses in the SC versus IN prime with SC or IN boost study. (A) CD-1 mice
 233 were untreated (n = 4) or received an SC prime, SC boost (n = 8); IN prime, IN boost (n = 7); or
 234 SC prime, IN boost (n = 8). (B) Sera levels of anti-S antibodies (dilution 1:30) by subtype are
 235 shown and (C) percent inhibition in the surrogate neutralization assay of ACE2:S RBD binding
 236 wherein inhibition of 35% or greater is associated with neutralization of viral infection. (D) Levels
 237 of anti-N IgG in sera (dilution 1:270). (E) Anti-S IgG by subtype (dilution 1:30) and (F)
 238 neutralization by lung homogenate. (G) Lung anti-N IgG levels (dilution 1:30). (H) Both anti-S
 239 and anti-N IgA in lung homogenate. (I) The Th1/Th2 ratios for sera and lung anti-S and anti-N
 240 antibodies where values greater than 1 represent Th1 dominance. Statistical analyses performed
 241 using One-way ANOVA with Tukey's post-hoc analysis comparing each group to every other
 242 group where *p < 0.05; **p ≤ 0.01; ***p ≤ 0.001; and ****p ≤ 0.0001.

243

244 **Both CD4+ and CD8+ T-cell responses were greater to N than S, and higher with SC delivery**

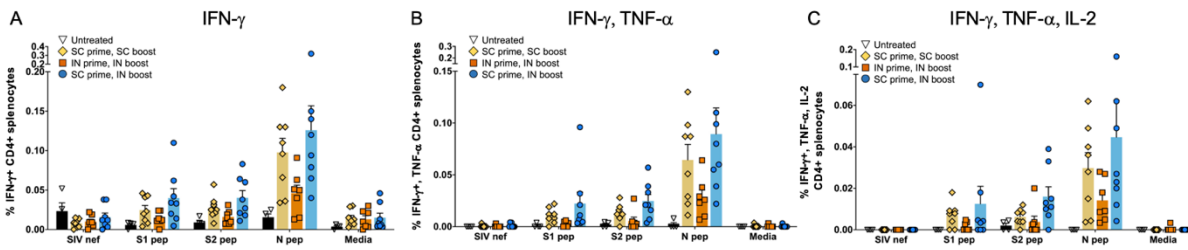
245 Intracellular cytokine staining (ICS) of IFN- γ (Fig. 4A, D); IFN- γ , TNF- α (Fig. 4B, E), and
246 IFN- γ , TNF- α , interleukin-2 (IL-2) (Fig. 4C, F) showed the highest mean values for the SC > SC
247 boost and SC > IN vaccinated groups with responses to the N peptide pool trending higher for both
248 CD4+ and CD8+ T cells. This was somewhat in contrast with the findings of the first SC > SC
249 boost study (study 1 above) where CD8+ T-cell responses were greater to the S1 peptide pool (Fig.
250 2C), however, variation is expected in outbred CD-1 mice and robust CD8+ responses to both S
251 and N were detected in SC > SC mice from each study. While the differences were not statistically
252 significant due to variation among individual mice, overall the IN > IN boost group had a reduced
253 population of CD8+ cells capable of accumulating IFN- γ (Fig. 4D) and IFN- γ + TNF- α (Fig. 4E)
254 in response to S and N peptide stimulation.

255 ELISpot findings were similar, with higher responses seen for the SC > SC and SC > IN
256 groups when compared to the IN > IN group, and the highest responses were found to be specific
257 to the N peptide pool (Fig. 4G). Interleukin-4 (IL-4) secretion in ELISpot was very low for all
258 groups (Fig. 4H), therefore the IFN- γ /IL-4 ratios were above 1 for almost all vaccinated mice in
259 response to both S and N peptide pools (Fig. 4I).

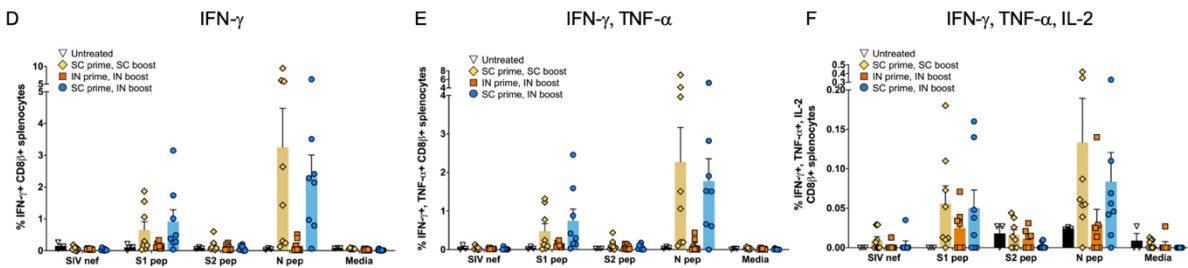
260 The T-cell responses in this study suggested an important contribution of SC delivery to T cell
261 responses.

The SC versus IN Prime with IN or SC Boost Study: T-cell Responses

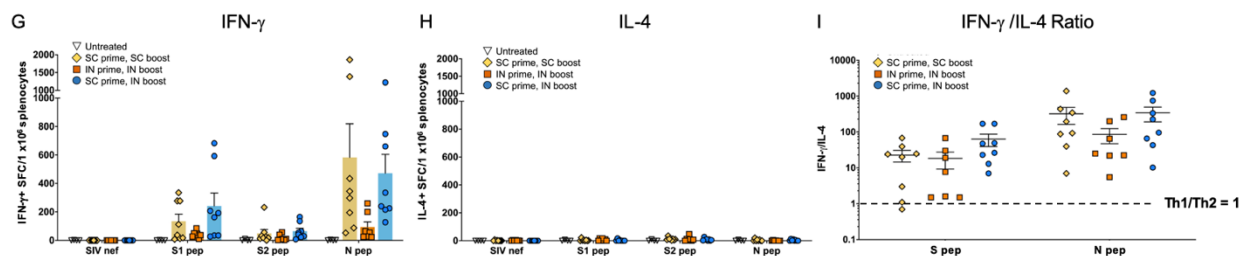
CD4+ ICS



CD8+ ICS



ELISpot



262 **Fig. 4** Both CD4+ and CD8+ T cells respond the nucleocapsid peptides in SC versus IN prime
 263 study with SC or IN boost. Cytokine production in response to S1, S2 and N peptide pools as
 264 detected by Intracellular cytokine staining (ICS) of (A) Interferon- γ (IFN- γ); (B) IFN- γ and tumor
 265 necrosis factor α (TNF- α); and (C) IFN- γ , TNF- α , and interleukin-2 (IL-2) production by CD4+
 266 is shown. ICS (D-F) IFN- γ ; IFN- γ , TNF- α ; and IFN- γ , TNF- α , and IL-2 for CD8+ T cells is shown.
 267 Some outliers by the Grubb's test were removed. ELISpot for (G) IFN- γ and (H) interleukin-4 (IL-
 268 4) secretion in response to the peptide pools is shown. SIV nef is a negative control. (I) The IFN-
 269 γ /IL-4 ratio showing T helper cell 1 dominance. Statistical analyses performed using One-way
 270 ANOVA with Dunnett's post-hoc comparison of each treatment group to untreated for each
 271 peptide pool was performed but did not reveal statistically significant differences due to individual
 272 variation amongst mice.
 273

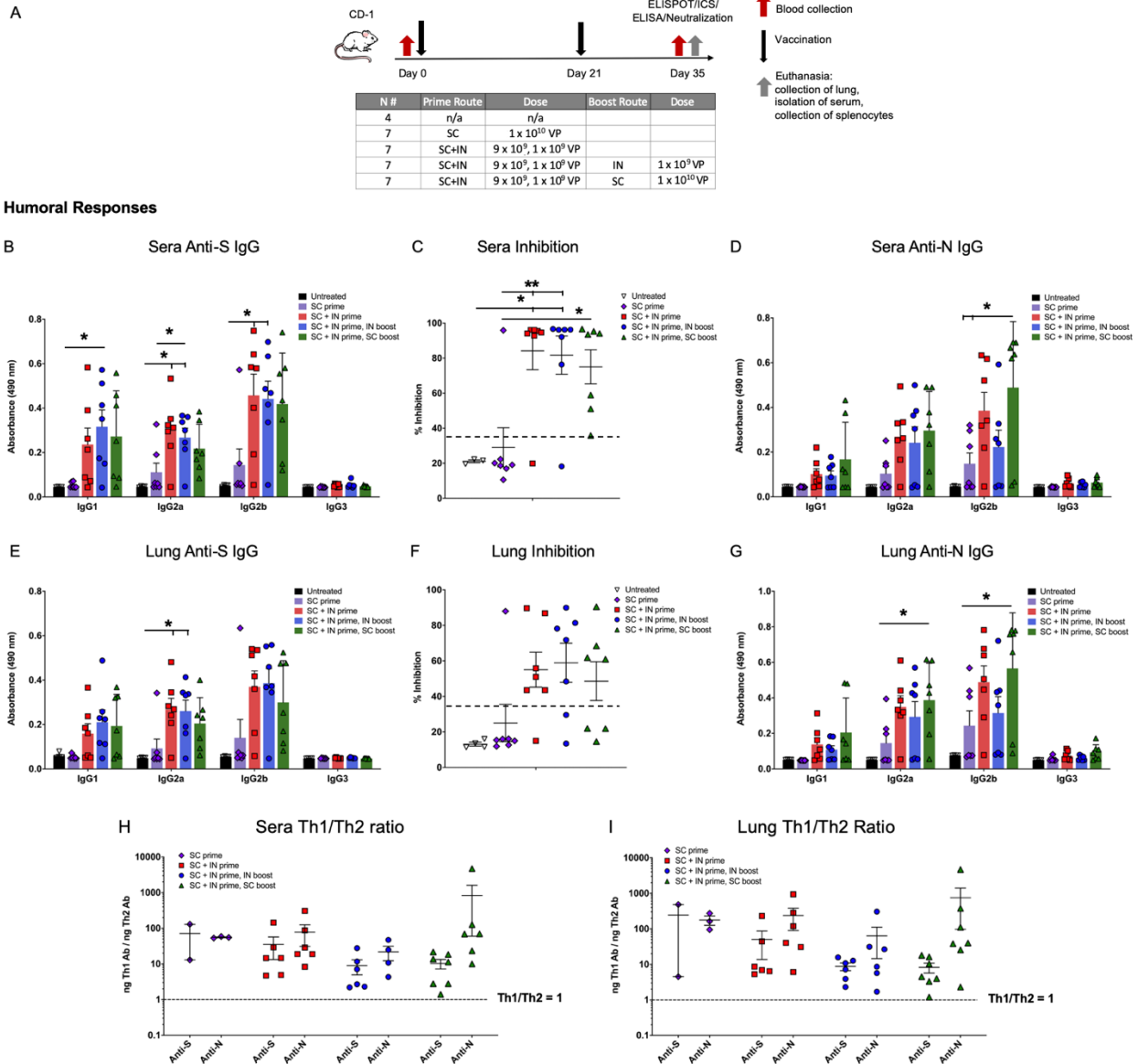
274
 275 **Prime-only delivery by combined SC and IN dosing elicits humoral responses that are as**
 276 **good or better than those with a boost**

277 To leverage both the humoral responses effectively elicited by IN delivery with the T-cell
 278 responses that were greater with SC delivery, we then tested prime delivery by a combination of

279 the SC and IN routes, with either IN or SC boosts. This study design is shown in Figure 5A. There
280 were 5 groups of CD-1 mice: untreated, an SC prime at 1×10^{10} viral particles (VP) without boost
281 (SC > no boost), a combined 9×10^9 VP SC plus 1×10^9 VP IN prime (SC/IN) without boost
282 (SC/IN > no boost), a combined SC/IN prime with 1×10^9 VP IN boost (SC/IN > IN), and a
283 combined SC/IN prime with a 1×10^{10} VP SC boost (SC/IN > SC). The untreated group was $n =$
284 4 and all vaccinated groups were $n = 7$. Mice received the prime on Day 0 and in appropriate
285 groups, the boost on Day 21. All mice were euthanized on Day 35 and tissue including blood for
286 serum, spleens for T cells, and lung tissue collected for analyses. Note this euthanasia day is one
287 week later than the two studies described above (Figs. 1A and 3A), which was a change meant to
288 better characterize humoral responses at a time point at which we expected cell-mediated responses
289 to remain high based on our prior work with this vaccine platform.

290 The combined SC/IN > no boost regimen was just as effective in eliciting neutralizing anti-S
291 IgG and anti-N IgG antibody production in both sera (Fig. 5B-D) and lung (Fig. 5E-G) as either
292 the SC/IN > IN or SC/IN > SC regimens. SC > no boost gave significantly lower humoral
293 responses (Fig. 5B-G). All humoral responses were Th1 dominant (Fig. 5H).

The Combined SC+IN Prime with IN or SC Boost study



294
 295 **Fig. 5** Subcutaneous (SC) plus intranasal (IN) prime without boost elicits Th1 dominant
 296 neutralizing anti-S and anti-N antibodies. (A) The study design is shown with groups for SC prime
 297 only, SC + IN prime only, and SC + IN prime with either an SC or IN boost, all n = 7. There was
 298 an untreated control group (n = 4). Prime dosing was on Day 0, boosts on Day 21, and euthanasia
 299 on Day 35. Shown are (B) serum anti-spike (S) antibodies by subtype (dilution 1:30); (C) %
 300 inhibition in the surrogate neutralization assay with sera (>35% is correlated with neutralization
 301 of virus); and (D) serum anti-nucleocapsid (N) antibodies (dilution 1:270). The same readouts (E)
 302 anti-S antibodies; (F) neutralization; and (G) anti-N antibodies are shown for lung homogenate
 303 (dilution 1:30 for anti-S and -N). The Th1/Th2 ratios for anti-S and anti-N antibodies are shown
 304 for (H) sera and (I) lung. Statistical analyses performed using One-way ANOVA with Tukey's
 305 post-hoc analysis comparing treatment groups within each antibody subtype or groups in the
 306 neutralization assay where *p < 0.05 and ** p ≤ 0.01.
 307

308 **SC plus IN prime alone without a boost elicits CD4+ T cell responses to N and CD8+ T-cell**
309 **responses to S**

310 Similar to the findings in the first study, ICS shows the N peptide pool stimulated cytokine
311 production by CD4+ T lymphocytes from all vaccinated mice (Fig. 6A-C), but CD8+ T cells from
312 vaccinated mice responded to S peptide pool 1 which contains the S RBD (Fig. 6D-F). The
313 differences between vaccinated groups were not significant due to variability amongst mice, with
314 SC/IN > no boost vaccinated mice having T-cell responses that were similar to those seen with
315 mice that did receive boosts.

316 In ELISpot, the highest IFN- γ secretion in response to peptide pools differed by both peptide
317 pool and vaccination regimen. As compared to the negative control (SIV nef), T cell IFN- γ
318 secretion was significantly greater for the combined SC/IN > SC group in response to the S1
319 peptide pool; greater for the SC/IN > IN group to the S2 peptide pool; and greater for the SC/IN >
320 no boost group to the N peptide pool (Fig. 6G).

321 IL-4 secretion was very low (Fig. 6H), therefore the IFN- γ /IL-4 ratio was above 1 for all
322 vaccinated mice with only one exception, reflecting Th1 dominance of T-cell responses (Fig. 6I).

323

324

325

326

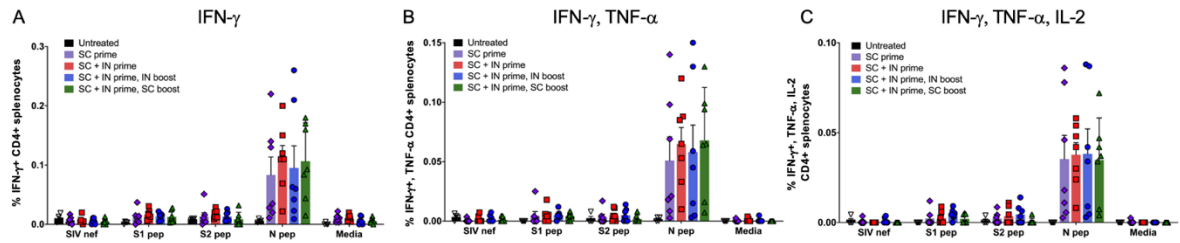
327

328

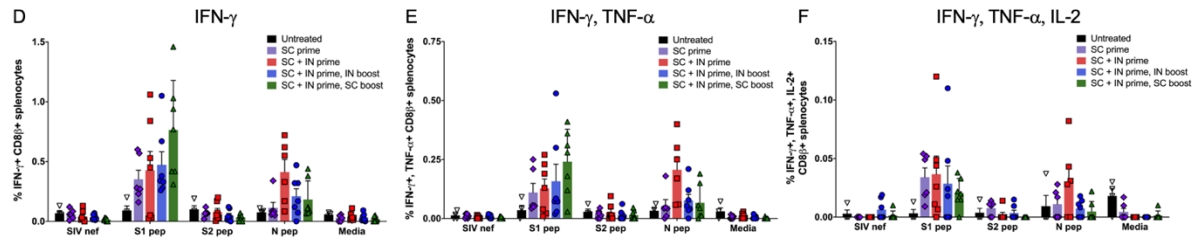
329

The **Combined SC+IN Prime with IN or SC Boost** study: T-Cell Responses

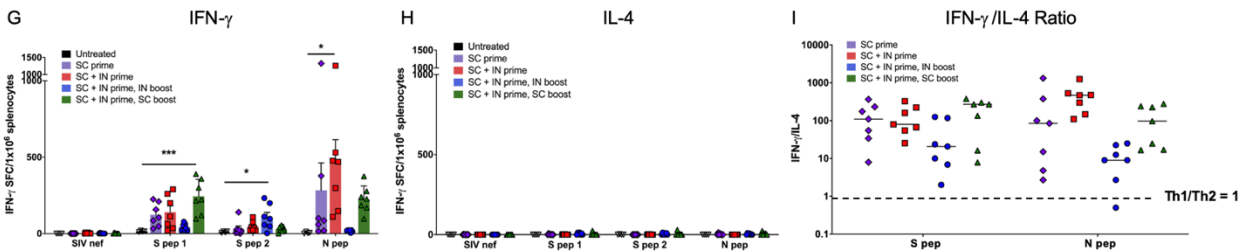
CD4+ ICS



CD8+ ICS



ELISpot



330
 331 **Fig. 6** CD4+ T-cells respond to nucleocapsid (N) and CD8+ T cells to the spike in the combined
 332 SC plus IN prime study with SC or IN boost. Interferon- γ (IFN- γ); IFN- γ and tumor necrosis factor
 333 α (TNF- α); and (C) IFN- γ , TNF- α , and interleukin-2 (IL-2) production by CD4+ (A-C) and CD8+
 334 (D-F) T-cells, respectively, in response to spike 1 (S1, containing the receptor binding domain),
 335 S2, and N peptide pools as detected by intracellular cytokine staining (ICS). Some outliers by the
 336 Grubb's test were removed. ELISpot for (G) IFN- γ and (H) interleukin-4 (IL-4) secretion in
 337 response to the peptide pools. SIV nef and media are negative controls. (I) The IFN- γ /IL-4 ratio
 338 showing T helper cell 1 dominance. Statistical analyses performed using One-way ANOVA with
 339 Dunnett's post-hoc comparison of each treatment group to untreated for each peptide pool where
 340 * $p < 0.05$, ** $p \leq 0.01$, and *** $p \leq 0.001$.
 341

342 **DISCUSSION**

343 Our hAd5 S-Fusion + N-ETSD vaccine was designed to overcome the risks of an S-only
 344 vaccine and elicit both T-cell immunity and neutralizing antibodies, leveraging the vital role T
 345 cells play in generating long-lasting antibody responses and in directly killing infected cells. The

346 CD4⁺ and CD8⁺ T cells responses induced by this vaccine are multifunctional, and induction of
347 such multifunctional T cells by vaccines is correlated with better protection against infection.⁴³
348 We posit that enhanced CD4⁺ T-cell responses and Th1 predominance resulting from expression
349 of an S antigen optimized for surface display and an N antigen optimized for endosomal/lysosomal
350 subcellular compartment localization and thus MHC I and II presentation, led to increased
351 dendritic cell presentation, cross-presentation, B cell activation, and ultimately high neutralization
352 capability. Furthermore, the potent neutralization capability at high dilution seen for sera from
353 hAd5 S-Fusion + N-ETSD vaccinated mice, combined with Th1 dominance of antibodies
354 generated in response to both S and N antigens, supports the objective of this vaccine design.

355 It is well established that the contemporaneous MHC I and MHC II presentation of an antigen
356 by the antigen presenting cell activates CD4⁺ and CD8⁺ T cells simultaneously and is optimal for
357 the generation of memory B and T cells. A key finding of our construct is that N-ETSD, which we
358 show is directed to the endosomal/lysosomal compartment, elicits a CD4⁺ response, a necessity
359 for induction of memory T cells and helper cells for B cell antibody production. Others have also
360 reported on the importance of lysosomal localization for eliciting the strongest T-cell IFN- γ and
361 CTL responses, compared to natural N.^{44,45}

362 The T-cell responses to the S and N antigens expressed by hAd5 S-Fusion + N-ETSD were
363 polycytokine, including IFN- γ , TNF- α , and IL-2 consistent with successful antimicrobial
364 immunity in bacterial and viral infections.⁴⁶⁻⁵⁰ Post-vaccination polycytokine T-cell responses
365 have been shown to correlate with vaccine efficacy, including those with a viral vector.⁴³ Highly
366 relevant here, polycytokine T-cell responses to SARS-CoV-2 N protein are consistent with
367 recovered COVID-19 patients,²⁰ suggesting that the bivalent hAd5 S-Fusion + N-ETSD vaccine
368 will provide vaccine subjects with greater protection against SARS-CoV-2.

369 The key finding here that prime-only vaccination delivered by combination SC and IN dosing
370 results in broad humoral and T-cell responses, with the potential for enhanced mucosal immunity,
371 supports the ongoing clinical testing of the hAd5 S-Fusion + N-ETSD. The vaccine has currently
372 completed Phase 1 testing as an SC prime and SC boost, and oral boost formulations that have
373 shown efficacy in the ability to elicit both humoral and T-cell responses that conferred complete
374 protection against high-titer SARS-CoV-2 challenge in our pre-clinical studies in non-human
375 primates, ¹ will soon also be tested in the clinic. To our knowledge, our vaccine is currently the
376 only one available in SC, thermally-stable oral,⁵¹ and IN formulations that offer the expanded
377 possibilities for efficient, feasible delivery across the globe, particularly in developing nations.

378

379 REFERENCES

- 380 1 Gabitzsch, E. *et al.* Complete Protection of Nasal and Lung Airways Against SARS-CoV-2
381 Challenge by Antibody Plus Th1 Dominant N- and S-Specific T-Cell Responses to
382 Subcutaneous Prime and Thermally-Stable Oral Boost Bivalent hAd5 Vaccination in an
383 NHP Study. *bioRxiv*, 2020.2012.2008.416297, doi:10.1101/2020.12.08.416297 (2021).
- 384 2 Sieling, P. *et al.* Th1 Dominant Nucleocapsid and Spike Antigen-Specific CD4+ and CD8+
385 Memory T Cell Recall Induced by hAd5 S-Fusion + N-ETSD Infection of Autologous
386 Dendritic Cells from Patients Previously Infected with SARS-CoV-2. *medRxiv*,
387 2020.2011.2004.20225417, doi:10.1101/2020.11.04.20225417 (2020).
- 388 3 Amalfitano, A., Begy, C. R. & Chamberlain, J. S. Improved adenovirus packaging cell lines
389 to support the growth of replication-defective gene-delivery vectors. *Proceedings of the*
390 *National Academy of Sciences of the United States of America* **93**, 3352-3356,
391 doi:10.1073/pnas.93.8.3352 (1996).
- 392 4 Amalfitano, A. *et al.* Production and Characterization of Improved Adenovirus Vectors
393 with the E1, E2b, and E3 Genes Deleted. *Journal of virology* **72**, 926,
394 doi:10.1128/JVI.72.2.926-933.1998 (1998).
- 395 5 Gatti-Mays, M. E. *et al.* A Phase I Trial Using a Multitargeted Recombinant Adenovirus 5
396 (CEA/MUC1/Brachyury)-Based Immunotherapy Vaccine Regimen in Patients with
397 Advanced Cancer. *Oncologist* **25**, 479, doi:10.1634/theoncologist.2019-0608 (2019).
- 398 6 Gabitzsch, E. S. *et al.* Anti-tumor immunotherapy despite immunity to adenovirus using
399 a novel adenoviral vector Ad5 [E1-, E2b-]-CEA. *Cancer Immunology, Immunotherapy* **59**,
400 1131-1135, doi:10.1007/s00262-010-0847-8 (2010).

- 401 7 Gabitzsch, E. S. & Jones, F. R. New recombinant SAd5 vector overcomes Ad5 immunity
402 allowing for multiple safe, homologous, immunizations. *J Clin Cell Immunol* **S4**, 001,
403 doi:doi:10.4172/2155-9899 (2011).
- 404 8 Gabitzsch, E. S. *et al.* Anti-tumor immunotherapy despite immunity to adenovirus using
405 a novel adenoviral vector Ad5 [E1-, E2b-]-CEA. *Cancer immunology, immunotherapy : CII*
406 **59**, 1131-1135, doi:10.1007/s00262-010-0847-8 (2010).
- 407 9 Wrapp, D. *et al.* Cryo-EM structure of the 2019-nCoV spike in the prefusion
408 conformation. *Science* **367**, 1260-1263, doi:10.1126/science.abb2507 (2020).
- 409 10 Lu, R. *et al.* Genomic characterisation and epidemiology of 2019 novel coronavirus:
410 implications for virus origins and receptor binding. *Lancet (London, England)* **395**, 565-
411 574, doi:10.1016/S0140-6736(20)30251-8 (2020).
- 412 11 Walls, A. C. *et al.* Structure, Function, and Antigenicity of the SARS-CoV-2 Spike
413 Glycoprotein. *Cell* **181**, 281-292.e286, doi:10.1016/j.cell.2020.02.058 (2020).
- 414 12 Hamming, I. *et al.* Tissue distribution of ACE2 protein, the functional receptor for SARS
415 coronavirus. A first step in understanding SARS pathogenesis. *J Pathol* **203**, 631-637,
416 doi:10.1002/path.1570 (2004).
- 417 13 Tai, W. *et al.* Characterization of the receptor-binding domain (RBD) of 2019 novel
418 coronavirus: implication for development of RBD protein as a viral attachment inhibitor
419 and vaccine. *Cell Mol Immunol*, doi:10.1038/s41423-020-0400-4 (2020).
- 420 14 Suthar, M. S. *et al.* Rapid generation of neutralizing antibody responses in COVID-19
421 patients. *Cell Reports Medicine*, doi:10.1016/j.xcrm.2020.100040.
- 422 15 Grifoni, A. *et al.* Targets of T Cell Responses to SARS-CoV-2 Coronavirus in Humans with
423 COVID-19 Disease and Unexposed Individuals. *Cell* **181**, 1489,
424 doi:10.1016/j.cell.2020.05.015 (2020).
- 425 16 Tegally, H. *et al.* Sixteen novel lineages of SARS-CoV-2 in South Africa. *Nature Medicine*,
426 doi:10.1038/s41591-021-01255-3 (2021).
- 427 17 Leung, K., Shum, M. H., Leung, G. M., Lam, T. T. & Wu, J. T. Early transmissibility
428 assessment of the N501Y mutant strains of SARS-CoV-2 in the United Kingdom, October
429 to November 2020. *Euro Surveill* **26**, doi:10.2807/1560-7917.Es.2020.26.1.2002106
430 (2021).
- 431 18 Davies, N. G. *et al.* Estimated transmissibility and severity of novel SARS-CoV-2 Variant
432 of Concern 202012/01 in England. *medRxiv*, 2020.2012.2024.20248822,
433 doi:10.1101/2020.12.24.20248822 (2020).
- 434 19 Zhang, W. *et al.* Emergence of a Novel SARS-CoV-2 Variant in Southern California. *JAMA*,
435 doi:10.1001/jama.2021.1612 (2021).
- 436 20 Peng, H. *et al.* Long-lived memory T lymphocyte responses against SARS coronavirus
437 nucleocapsid protein in SARS-recovered patients. *Virology* **351**, 466-475,
438 doi:<https://doi.org/10.1016/j.virol.2006.03.036> (2006).
- 439 21 Shang, B. *et al.* Characterization and application of monoclonal antibodies against N
440 protein of SARS-coronavirus. *Biochemical and Biophysical Research Communications*
441 **336**, 110-117, doi:<https://doi.org/10.1016/j.bbrc.2005.08.032> (2005).
- 442 22 Azizi, A. *et al.* A combined nucleocapsid vaccine induces vigorous SARS-CD8+ T-cell
443 immune responses. *Genet Vaccines Ther* **3**, 7, doi:10.1186/1479-0556-3-7 (2005).

- 444 23 Zeng, W. *et al.* Biochemical characterization of SARS-CoV-2 nucleocapsid protein.
445 *Biochemical and biophysical research communications*, S0006-0291X(0020)30876-
446 30877, doi:10.1016/j.bbrc.2020.04.136 (2020).
- 447 24 Narayanan, K., Chen, C.-J., Maeda, J. & Makino, S. Nucleocapsid-independent specific
448 viral RNA packaging via viral envelope protein and viral RNA signal. *Journal of virology*
449 **77**, 2922-2927, doi:10.1128/jvi.77.5.2922-2927.2003 (2003).
- 450 25 McBride, R., van Zyl, M. & Fielding, B. C. The coronavirus nucleocapsid is a
451 multifunctional protein. *Viruses* **6**, 2991-3018, doi:10.3390/v6082991 (2014).
- 452 26 Nisreen, M. A. O. *et al.* Severe Acute Respiratory Syndrome Coronavirus 2-Specific
453 Antibody Responses in Coronavirus Disease 2019 Patients. *Emerging Infectious Disease*
454 *journal* **26**, 1478-1488, doi:10.3201/eid2607.200841 (2020).
- 455 27 Long, Q.-X. *et al.* Antibody responses to SARS-CoV-2 in patients with COVID-19. *Nature*
456 *Medicine*, doi:10.1038/s41591-020-0897-1 (2020).
- 457 28 Altmann, D. M. & Boyton, R. J. SARS-CoV-2 T cell immunity: Specificity, function,
458 durability, and role in protection. *Sci Immunol* **5**, doi: 10.1126/sciimmunol.abd6160,
459 doi:10.1126/sciimmunol.abd6160 (2020).
- 460 29 Ni, L. *et al.* Detection of SARS-CoV-2-Specific Humoral and Cellular Immunity in COVID-
461 19 Convalescent Individuals. *Immunity*, doi:10.1016/j.immuni.2020.04.023 (2020).
- 462 30 Weiskopf, D. *et al.* Phenotype and kinetics of SARS-CoV-2-specific T cells in COVID-19
463 patients with acute respiratory distress syndrome. *Science Immunology* **5**, eabd2071,
464 doi:10.1126/sciimmunol.abd2071 (2020).
- 465 31 Ng, O. W. *et al.* Memory T cell responses targeting the SARS coronavirus persist up to 11
466 years post-infection. *Vaccine* **34**, 2008-2014, doi:10.1016/j.vaccine.2016.02.063 (2016).
- 467 32 Tang, F. *et al.* Lack of peripheral memory B cell responses in recovered patients with
468 severe acute respiratory syndrome: a six-year follow-up study. *Journal of immunology*
469 (*Baltimore, Md. : 1950*) **186**, 7264-7268, doi:10.4049/jimmunol.0903490 (2011).
- 470 33 Le Bert, N. *et al.* SARS-CoV-2-specific T cell immunity in cases of COVID-19 and SARS, and
471 uninfected controls. *Nature* **584**, 457, doi:10.1038/s41586-020-2550-z (2020).
- 472 34 Sekine, T. *et al.* Robust T cell immunity in convalescent individuals with asymptomatic or
473 mild COVID-19. *Cell* **183**, 158, doi:10.1101/2020.06.29.174888 (2020).
- 474 35 Vabret, N. Antibody responses to SARS-CoV-2 short-lived. *Nature Reviews Immunology*,
475 doi:10.1038/s41577-020-0405-3 (2020).
- 476 36 Polack, F. P. *et al.* Safety and Efficacy of the BNT162b2 mRNA Covid-19 Vaccine. *N Engl J*
477 *Med* **383**, 2603-2615, doi:10.1056/NEJMoa2034577 (2020).
- 478 37 Baden, L. R. *et al.* Efficacy and Safety of the mRNA-1273 SARS-CoV-2 Vaccine. *N Engl J*
479 *Med* **384**, 403-416, doi:10.1056/NEJMoa2035389 (2021).
- 480 38 Magrone, T., Magrone, M. & Jirillo, E. Focus on Receptors for Coronaviruses with Special
481 Reference to Angiotensin- Converting Enzyme 2 as a Potential Drug Target - A
482 Perspective. *Endocr Metab Immune Disord Drug Targets* **20**, 807-811,
483 doi:10.2174/1871530320666200427112902 (2020).
- 484 39 Fehr, A. R. & Perlman, S. Coronaviruses: an overview of their replication and
485 pathogenesis. *Methods in molecular biology (Clifton, N.J.)* **1282**, 1-23, doi:10.1007/978-
486 1-4939-2438-7_1 (2015).

- 487 40 Bourouiba, L. Turbulent Gas Clouds and Respiratory Pathogen Emissions: Potential
488 Implications for Reducing Transmission of COVID-19. *Jama* **323**, 1837-1838,
489 doi:10.1001/jama.2020.4756 (2020).
- 490 41 Sterlin, D. *et al.* IgA dominates the early neutralizing antibody response to SARS-CoV-2.
491 *Sci Transl Med* **13**, doi:10.1126/scitranslmed.abd2223 (2021).
- 492 42 Tan, C. W. *et al.* A SARS-CoV-2 surrogate virus neutralization test based on antibody-
493 mediated blockage of ACE2-spike protein-protein interaction. *Nat Biotechnol* **38**, 1073-
494 1078, doi:10.1038/s41587-020-0631-z (2020).
- 495 43 Darrah, P. A. *et al.* Multifunctional TH1 cells define a correlate of vaccine-mediated
496 protection against *Leishmania major*. *Nat Med* **13**, 843-850, doi:10.1038/nm1592
497 (2007).
- 498 44 Gupta, V. *et al.* SARS coronavirus nucleocapsid immunodominant T-cell epitope cluster
499 is common to both exogenous recombinant and endogenous DNA-encoded
500 immunogens. *Virology* **347**, 127-139, doi:10.1016/j.virol.2005.11.042 (2006).
- 501 45 Yang, K. *et al.* Immune responses to T-cell epitopes of SARS CoV-N protein are enhanced
502 by N immunization with a chimera of lysosome-associated membrane protein. *Gene*
503 *Ther* **16**, 1353-1362, doi:10.1038/gt.2009.92 (2009).
- 504 46 Lichterfeld, M. *et al.* HIV-1-specific cytotoxicity is preferentially mediated by a subset of
505 CD8(+) T cells producing both interferon-gamma and tumor necrosis factor-alpha. *Blood*
506 **104**, 487-494, doi:10.1182/blood-2003-12-4341 (2004).
- 507 47 Betts, M. R. *et al.* HIV nonprogressors preferentially maintain highly functional HIV-
508 specific CD8+ T cells. *Blood* **107**, 4781-4789, doi:10.1182/blood-2005-12-4818 (2006).
- 509 48 Cox, M. A. & Zajac, A. J. Shaping successful and unsuccessful CD8 T cell responses
510 following infection. *J Biomed Biotechnol* **2010**, 159152-159152,
511 doi:10.1155/2010/159152 (2010).
- 512 49 Rosendahl Huber, S., van Beek, J., de Jonge, J., Luytjes, W. & van Baarle, D. T cell
513 responses to viral infections - opportunities for Peptide vaccination. *Front Immunol* **5**,
514 171-171, doi:10.3389/fimmu.2014.00171 (2014).
- 515 50 Seder, R. A., Darrah, P. A. & Roederer, M. T-cell quality in memory and protection:
516 implications for vaccine design. *Nat Rev Immunol* **8**, 247-258, doi:10.1038/nri2274
517 (2008).
- 518 51 Stewart, M., Ward, S. J. & Drew, J. Use of adenovirus as a model system to illustrate a
519 simple method using standard equipment and inexpensive excipients to remove live
520 virus dependence on the cold-chain. *Vaccine* **32**, 2931-2938,
521 doi:10.1016/j.vaccine.2014.02.033 (2014).
- 522 52 Zhu, F.-C. *et al.* Safety, tolerability, and immunogenicity of a recombinant adenovirus
523 type-5 vectored COVID-19 vaccine: a dose-escalation, open-label, non-randomised, first-
524 in-human trial. *The Lancet*, doi:10.1016/S0140-6736(20)31208-3.
- 525 53 van Doremalen, N. *et al.* ChAdOx1 nCoV-19 vaccination prevents SARS-CoV-2
526 pneumonia in rhesus macaques. *bioRxiv*, 2020.2005.2013.093195,
527 doi:10.1101/2020.05.13.093195 (2020).
- 528 54 Amalfitano, A. & Chamberlain, J. S. Isolation and characterization of packaging cell lines
529 that coexpress the adenovirus E1, DNA polymerase, and preterminal proteins:
530 implications for gene therapy. *Gene Ther* **4**, 258-263, doi:10.1038/sj.gt.3300378 (1997).

- 531 55 Seregin, S. S. & Amalfitano, A. Overcoming pre-existing adenovirus immunity by genetic
532 engineering of adenovirus-based vectors. *Expert Opin Biol Ther* **9**, 1521-1531,
533 doi:10.1517/14712590903307388 (2009).
- 534 56 Srinivasan, S. *et al.* Structural Genomics of SARS-CoV-2 Indicates Evolutionary Conserved
535 Functional Regions of Viral Proteins. *Viruses* **12**, 360, doi:10.3390/v12040360 (2020).
- 536 57 Schaack, J. *et al.* Promoter strength in adenovirus transducing vectors: down-regulation
537 of the adenovirus E1A promoter in 293 cells facilitates vector construction. *Virology* **291**,
538 101-109, doi:10.1006/viro.2001.1211 (2001).
- 539 58 Tan, C. W. *et al.* A SARS-CoV-2 surrogate virus neutralization test based on antibody-
540 mediated blockage of ACE2-spike protein-protein interaction. *Nat Biotechnol*,
541 doi:10.1038/s41587-020-0631-z (2020).
- 542

543

544

545

546

547

548

549

550

551

552

553

554

555

556

557

558

559

560 **SUPPLEMENTARY INFORMATION**

561

562 **METHODS**

563

564 *The hAd5 [E1-, E2b-, E3-] platform and constructs*

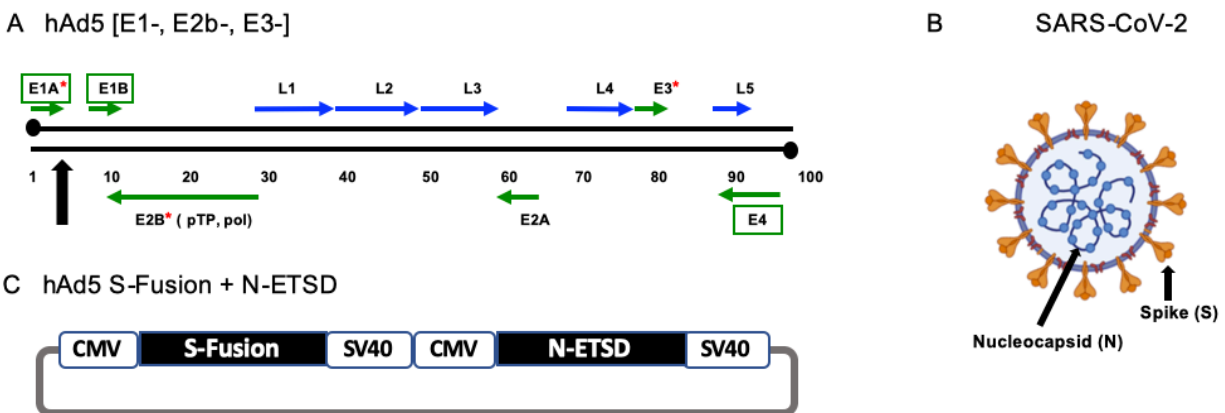
565

566 For studies here, the next generation hAd5 [E1-, E2b-, E3-] vector was used (Fig. S1A) to
567 create viral vaccine candidate constructs. This hAd5 [E1-, E2b-, E3-] vector is primarily
568 distinguished from other first-generation [E1-, E3-] recombinant Ad5 platforms^{52,53} by having
569 additional deletions in the early gene 2b (E2b) region that remove the expression of the viral DNA
570 polymerase (pol) and in pre terminal protein (pTP) genes, and its propagation in the E.C7 human
571 cell line.^{3,4,54,55}

572 The hAd5 S-Fusion + N-ETSD vaccine we utilized the hAd5 [E1-, E2b-, E3-] comprises a
573 wildtype spike (S) sequence [accession number YP009724390] modified with a proprietary linker
574 peptide sequence as well as a wildtype nucleocapsid (N) sequence [accession number
575 YP009724397] with a an Enhanced T-cell Stimulation Domain (ETSD) signal sequence to direct
576 translated N to the endosomal/lysosomal pathway.² The SARS-CoV-2 S protein is found on the
577 viral surface¹¹ and the N protein is found in the interior of the virus^{23,56} (Fig. S1B).

578 The powerful cytomegalovirus (CMV) promoter⁵⁷ drives expression in the hAd5 construct
579 (Fig. S1C).

580



581

582 **Fig. S1** *The SARS-CoV-2 virus, the hAd5 [E1-, E2b-, E3-] vector and the dual antigen hAd5 S-*
583 *Fusion + N-ETSD vaccine.* (A) The second-generation human adenovirus serotype 5 (hAd5)
584 vector used has the E1, E2b, and E3 regions deleted. Sequences for the vaccine antigen cargo are
585 inserted at the black arrow. (B) The spike (S) glycoprotein is displayed as a trimer on the surface
586 of SARS-CoV-2 and the nucleocapsid (N) protein is found in the virus interior, associated with
587 the viral RNA. (C) The vaccine antigens are under control of the cytomegalovirus (CMV) promoter
588 and sequences end with SV40 poly-A.

589

590 *Transfection of HEK 293T cells with hAd5 constructs and flow cytometric analysis of RBD*
591 *surface expression*

592

593 To determine surface expression of the RBD epitope by vaccine candidate constructs, we
594 transfected HEK 293T cells with hAd5 construct DNA and quantified surface RBD by flow
595 cytometric detection using anti-RBD antibodies. The constructs tested were: S-WT, S-WT + N-

596 ETSD, S-Fusion, S-Fusion + N-ETSD, and N-ETSD. HEK 293T cells (2.5×10^5 cells/well in 24
597 well plates) were grown in DMEM (Gibco Cat# 11995-065) with 10% FBS and 1X PSA (100
598 units/mL penicillin, 100 $\mu\text{g}/\text{mL}$ streptomycin, 0.25 $\mu\text{g}/\text{mL}$ Amphotericin B) at 37°C. Cells were
599 transfected with 0.5 μg of hAd5 plasmid DNA using a JetPrime transfection reagent (Polyplus
600 Catalog # 89129-924) according to the manufacturer's instructions. Cells were harvested 1, 2, 3,
601 and 7 days post transfection by gently pipetting cells into medium and labeled with an anti-RBD
602 monoclonal antibody (clone D003 Sino Biological Catalog # 40150-D003) and F(ab')₂-Goat anti-
603 Human IgG-Fc secondary antibody conjugated with R-phycoerythrin (ThermoFisher Catalog #
604 H10104). Labeled cells were acquired using a Thermo-Fisher Attune NxT flow cytometer and
605 analyzed using Flowjo Software.

606

607 *ACE2-IgG1Fc binding to hAd5 transfected HEK 293T cells*

608

609 HEK 293T cells were cultured at 37°C under conditions described above for transfection with
610 hAd5 S-WT, S-Fusion, and S-Fusion + N-ETSD and were incubated for 2 days and harvested for
611 ACE2-Fc binding analysis. Recombinant ACE2-IgG1Fc protein was produced using Maxcyte
612 transfection in CHO-S cells that were cultured for 14 days. ACE2-IgG1Fc was then purified using
613 a MabSelect SuRe affinity column on AKTA Explorer. Purified ACE2-IgG1Fc was dialyzed into
614 10 mM HEPES, pH7.4, 150 mM NaCl and concentrated to 2.6 mg/mL. For binding studies, the
615 ACE2-IgG1Fc was used at a concentration of 1 $\mu\text{g}/\text{mL}$ for binding. Cells were incubated with
616 ACE2-Fc for 20 minutes and, after a washing step, were then labeled with a PE conjugated F(ab')₂-
617 goat anti-human IgG Fc secondary antibody at a 1:100 dilution, incubated for 20 minutes, washed
618 and acquired on flow cytometer. Histograms are based on normalized mode (NM) of cell count –
619 count of cells positive for signal in PE channel.

620

621 *Murine immunization and blood/tissue collection*

622

623 CD-1 female mice (Charles River Laboratories) 6-8 weeks of age were used for
624 immunological studies performed at the vivarium facilities of Omeros Inc. (Seattle, WA). Mice
625 were administered subcutaneous (SC) injections at the indicated doses in 50 μL ARM buffer (20
626 mM Tris pH 8.0, 25 mM NaCl, with 2.5% glycerol) or intranasal (IN) injections at the indicated
627 doses in 10 μL ARM buffer (5 μL per nostril) while under isoflurane anesthesia. On the final day
628 of each study, blood was collected via the submandibular vein from isoflurane-anesthetized mice
629 for isolation of sera using a microtainer tube and then mice were euthanized for collection of spleen
630 and lungs.

631 Spleens were removed from each mouse and placed in 5 mL of sterile media
632 (RPMI/HEPES/Pen/Strep/10% FBS). Splenocytes were isolated within 2 hours of collection and
633 used fresh or frozen for later analysis.

634 Lungs were removed from each mouse, dissected in half and then immediately snap frozen
635 on dry ice. Lung homogenates were generated by thawing one frozen lung half and homogenizing
636 in 150 μL sterile PBS using a Fisher Scientific pestle drill. Homogenates were centrifuged at
637 13,000 rpm for 3 minutes and supernatants were utilized in ELISA and cPass surrogate
638 neutralization assays.

639

640 *Intracellular cytokine stimulation (ICS)*

641

642 ICS assays were performed using 10^6 live splenocytes per well in 96-well U-bottom plates.
643 Splenocytes in RPMI media supplemented with 10% FBS were stimulated by the addition of pools
644 of overlapping peptide for S or N antigens at 2 $\mu\text{g}/\text{mL}$ /peptide for 6 h at 37°C in 5% CO_2 , with
645 protein transport inhibitor, GolgiStop (BD) added two hours after initiation of incubation. The S
646 peptide pool (JPT: Cat #PM-WCPV-S-1) is a total of 315 spike peptides split into two pools
647 comprised of 158 and 157 peptides each. The N peptide pool (JPT; Cat # PM-WCPV-NCAP-1)
648 was also used to stimulate cells. A SIV-Nef peptide pool (BEI Resources) was used as an off-target
649 negative control. Stimulated splenocytes were then stained for a fixable cell viability stain
650 followed by the lymphocyte surface markers CD8 β and CD4, fixed with CytoFix (BD),
651 permeabilized, and stained for intracellular accumulation of IFN- γ , TNF- α and IL-2 (in studies 2
652 and 3). Fluorescent-conjugated antibodies against mouse CD8 β antibody (clone H35-17.2,
653 ThermoFisher), CD4 (clone RM4-5, BD), IFN- γ (clone XMG1.2, BD), TNF- α (clone MP6-XT22,
654 BD) and IL-2 (clone JES6-5H4; BD), and staining was performed in the presence of unlabeled
655 anti-CD16/CD32 antibody (clone 2.4G2; BD). Flow cytometry was performed using a Beckman-
656 Coulter Cytoflex S flow cytometer and analyzed using Flowjo Software.

657

658 *ELISpot assay*

659

660 ELISpot assays were used to detect cytokines secreted by splenocytes from inoculated mice.
661 Fresh splenocytes were used on the same day, as were cryopreserved splenocytes containing
662 lymphocytes. The cells ($2\text{-}4 \times 10^5$ cells per well of a 96-well plate) were added to the ELISpot
663 plate containing an immobilized primary antibodies to either IFN- γ or IL-4 (BD), and were
664 exposed to various stimuli (e.g. control peptides, target peptide pools/proteins) comprising 2
665 $\mu\text{g}/\text{mL}$ peptide pools or 10 $\mu\text{g}/\text{mL}$ protein for 36-40 hours. After aspiration and washing to remove
666 cells and media, extracellular cytokine was detected by a secondary antibody to cytokine
667 conjugated to biotin (BD). A streptavidin/horseradish peroxidase conjugate was used detect the
668 biotin-conjugated secondary antibody. The number of spots per well, or per $2\text{-}4 \times 10^5$ cells, was
669 counted using an ELISpot plate reader. A Th1/Th2 ratio was calculated by dividing the IFN- γ spot
670 forming cells (SFC) per million splenocytes with the IL-4 SFC per million splenocytes for each
671 animal.

672

673 *ELISA for detection of antibodies*

674

675 For IgG antibody detection in sera and lung homogenate from inoculated mice, ELISAs
676 specific for spike and nucleocapsid antibodies, as well as for IgG subtype (IgG1, IgG2a, IgG2b,
677 and IgG3) antibodies were used. In addition, for IgA antibody detection in lung homogenate from
678 inoculated mice, ELISAs specific for spike and nucleocapsid antibodies, as well as for IgA was
679 used. A microtiter plate was coated overnight with 100 ng of either purified recombinant SARS-
680 CoV-2 S-FTD (full-length S with fibrin trimerization domain, constructed and purified in-house
681 by ImmunityBio), SARS-CoV-2 S RBD (Sino Biological, Beijing, China; Cat # 401591-V08B1-
682 100) or purified recombinant SARS-CoV-2 nucleocapsid (N) protein (Sino Biological, Beijing,
683 China; Cat # 40588-V08B) in 100 μL of coating buffer (0.05 M Carbonate Buffer, pH 9.6). The
684 wells were washed three times with 250 μL PBS containing 1% Tween 20 (PBST) to remove
685 unbound protein and the plate was blocked for 60 minutes at room temperature with 250 μL PBST.
686 After blocking, the wells were washed with PBST, 100 μL of either diluted serum or diluted lung
687 homogenate samples were added to wells, and samples incubated for 60 minutes at room
688 temperature. After incubation, the wells were washed with PBST and 100 μL of a 1/5000 dilution

689 of anti-mouse IgG HRP (GE Health Care; Cat # NA9310V), or anti-mouse IgG₁ HRP (Sigma; Cat
690 # SAB3701171), or anti-mouse IgG_{2a} HRP (Sigma; Cat # SAB3701178), or anti-mouse IgG_{2b} HRP
691 (Sigma; catalog# SAB3701185), anti-mouse IgG₃ HRP conjugated antibody (Sigma; Cat #
692 SAB3701192), or anti-mouse IgA HRP conjugated antibody (Sigma; Cat # A4789) was added to
693 wells. For positive controls, a 100 µL of a 1/5000 dilution of rabbit anti-N IgG Ab or 100 µL of a
694 1/25 dilution of mouse anti-S serum (from mice immunized with purified S antigen in adjuvant)
695 were added to appropriate wells. After incubation at room temperature for 1 hour, the wells were
696 washed with PBS-T and incubated with 200 µL o-phenylenediamine-dihydrochloride (OPD
697 substrate (Thermo Scientific Cat # A34006) until appropriate color development. The color
698 reaction was stopped with addition of 50 µL 10% phosphoric acid solution (Fisher Cat # A260-
699 500) in water and the absorbance at 490 nm was determined using a microplate reader (SoftMax®
700 Pro, Molecular Devices).

701

702 *Calculation of relative ng amounts of antibodies and the Th1/Th2 ratio*

703

704 A standard curve of IgG was generated and absorbance values were converted into mass
705 equivalents for both anti-S and anti-N antibodies. Using these values, we were able to calculate
706 that hAd5 S-Fusion + N-ETSD vaccination generated a geometric mean value for S- and N-
707 specific IgG per milliliter of serum. These values were also used to generate a Th1/Th2 ratio for
708 the humoral responses by dividing the sum total of Th1 skewed antigen-specific IgG isotypes
709 (IgG_{2a}, IgG_{2b} and IgG₃) with the total Th2 skewed IgG₃, for each mouse. Some responses,
710 particularly for anti-N responses in IgG_{2a} and IgG_{2b} (both Th1 skewed isotypes), were above the
711 limit of quantification with OD values higher than those observed in the standard curve. These
712 data points were reduced to values within the standard curve, and thus will reflect a lower Th1/Th2
713 skewing than would otherwise be reported.

714

715 *cPassTM neutralizing antibody detection*

716

717 The GenScript cPassTM ([https://www.genscript.com/cpass-sars-cov-2-neutralization-
718 antibody-detection-Kit.html](https://www.genscript.com/cpass-sars-cov-2-neutralization-antibody-detection-Kit.html)) for detection of neutralizing antibodies was used according to the
719 manufacturer's instructions.⁵⁸ The kit detects circulating neutralizing antibodies against SARS-
720 CoV-2 that block the interaction between the S RBD with the ACE2 cell surface receptor. It is
721 suitable for all antibody isotypes and appropriate for use with in animal models without
722 modification.

723

724 *Vero E6 cell neutralization assay*

725

726 All aspects of the assay utilizing virus were performed in a BSL3 containment facility
727 according to the ISMMS Conventional Biocontainment Facility SOPs for SARS-CoV-2 cell
728 culture studies. Vero e6 kidney epithelial cells from *Cercopithecus aethiops* (ATCC CRL-1586)
729 were plated at 20,000 cells/well in a 96-well format and 24 hours later, cells were incubated with
730 antibodies or heat inactivated sera previously serially diluted in 3-fold steps in DMEM containing
731 2% FBS, 1% NEAAs, and 1% Pen-Strep; the diluted samples were mixed 1:1 with SARS-CoV-2
732 in DMEM containing 2% FBS, 1% NEAAs, and 1% Pen-Strep at 10,000 TCID₅₀/mL for 1 hr. at
733 37°C, 5% CO₂. This incubation did not include cells to allow for neutralizing activity to occur
734 prior to infection. The samples for testing included sera from the four mice that showed anti-S
735 IgG_{2a} and IgG_{2b} antibody responses in Fig. 1B, pooled sera from those four mice, sera from a

736 COVID-19 convalescent patient, and media only. For detection of neutralization, 120 μ L of the
737 virus/sample mixture was transferred to the Vero E6 cells and incubated for 48 hours before
738 fixation with 4% PFA. Each well received 60 μ L of virus or an infectious dose of 600 TCID₅₀.
739 Control wells including 6 wells on each plate for no virus and virus-only controls were used. The
740 percent neutralization was calculated as $100 - ((\text{sample of interest} - [\text{average of "no virus"}]) / [\text{average}$
741 $\text{of "virus only"}]) * 100$) with a stain for CoV-2 Np imaged on a Celigo Imaging Cytometer
742 (Nexcelom Bioscience).

743

744 **SUPPLEMENTARY RESULTS**

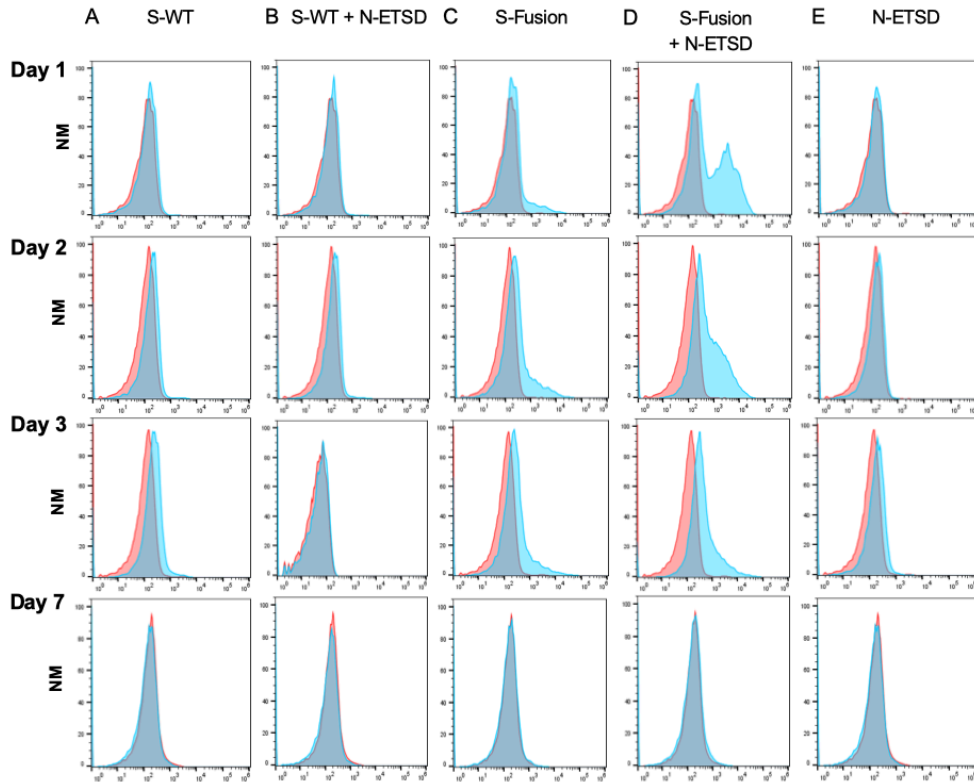
745

746 **Enhanced HEK 293T cell-surface expression of RBD following transfection with Ad5 S-** 747 **Fusion + N-ETSD**

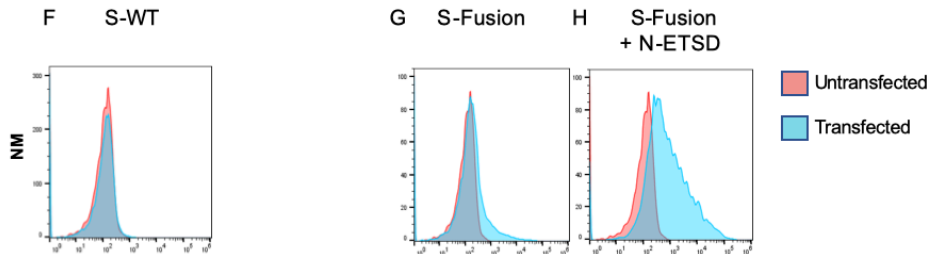
748

749 As shown in Figure S2, anti-RBD-specific antibodies did not detect RBD on the surface of
750 HEK 293T cells transfected with hAd5 S-WT (Fig. 2A) or hAd5 S-WT + N-ETSD (Fig. 2B)
751 constructs, while hAd5 S-Fusion alone was higher (Fig. 2C). Notably, the highest cell-surface
752 expression of RBD was detected after transfection with dual antigen hAd5 S-Fusion + N-ETSD
753 (Fig. 2D). Similar results were seen for recombinant ACE2-Fc binding to S-WT, S-Fusion and S-
754 Fusion + N-ETSD, with ACE2 showing higher binding to S-Fusion than S-WT and the dual
755 antigen construct showing the highest binding (Fig. S2F-H). These findings support our
756 proposition that an hAd5 S-Fusion + N-ETSD construct, containing a high number and variety of
757 antigens provided by both full-length, optimized S with proper folding and N leads to enhanced
758 expression and cell surface display of RBD in a vaccine construct.
759

Anti-RBD Antibody



ACE2-Fc



760
761 **Fig. S2** Transfection of HEK293T cells with hAd5 S-Fusion + ETSD results in enhanced surface
762 expression of the spike receptor binding domain (RBD). Flow cytometric analysis of an anti-RBD
763 antibody with construct-transfected cells reveals no detectable surface expression of RBD in either
764 (A) S-WT or (B) S-WT + N-ETSD transfected cells. Expression was higher in (C) S-Fusion
765 transfected cells as compared to S-WT. Cell surface expression of the RBD was high in (D) S-
766 Fusion + N-ETSD transfected cells, particularly at day 1 and 2. (E) No expression was detected
767 the N-ETSD negative control. Recombinant ACE2-Fc binding to (F) S-WT, (G) and S-Fusion, and
768 (H) S-Fusion + N-ETSD is shown. Y-axis scale is normalized to mode (NM).